

On the non-monotonic field-dependence of the ZFC magnetization peak in some systems of magnetic nanoparticles

R. Sappey, E. Vincent, N. Hadacek

*Service de Physique de l'Etat Condensé, CEA Saclay,
91191 Gif sur Yvette Cedex, France*

F. Chaput, J.P. Boilot,

*Groupe de Chimie des Solides, Laboratoire P.M.C., CNRS URA D1254,
Ecole Polytechnique, 91128 Palaiseau, France*

D. Zins,

*Laboratoire de Physico-Chimie, CNRS ER 44,
Université Pierre et Marie Curie, 4 place Jussieu, 75252 Paris, France*

Abstract

We have performed magnetic measurements on a diluted system of $\gamma - Fe_2O_3$ nanoparticles ($d \sim 7nm$), and on a ferritin sample. In both cases, the ZFC-peak presents a non-monotonic field dependence, as has already been reported in some experiments, and discussed as a possible evidence of resonant tunneling. Within simple assumptions, we derive expressions for the magnetization obtained in the usual ZFC, FC, TRM procedures. We point out that the ZFC-peak position is extremely sensitive to the width of the particle size distribution, and give some numerical estimates of this effect. We propose another experimental procedure, which combines the FC magnetization with a modified TRM measurement, and allows a more direct access to the barrier distribution in a field. The typical barrier values which are obtained in this procedure show a monotonic decrease for increasing fields, as expected from the simple effect of anisotropy barrier lowering, in contrast with the ZFC results. From our measurements on $\gamma - Fe_2O_3$ particles, we show that the width of the effective barrier distribution is slightly increasing with the field, an effect which is sufficient for causing the observed initial increase of the ZFC-peak temperatures.

P.A.C.S. numbers : 75.50.Tt, 75.45.+j, 75.60.Nt

E-mail: sappey@spec.saclay.cea.fr, vincent@spec.saclay.cea.fr

1 Introduction

A rapid characterization of ensembles of small magnetic particles (like ferrofluids) is very commonly achieved by “zero-field cooled” (ZFC) magnetization measurements. The ZFC curve is measured by cooling the sample in zero field, applying the field at low temperature and then measuring the magnetization while raising the temperature by steps. The ZFC curve peaks at a temperature which is related to a typical scale of the anisotropy energy barriers in the system; it is commonly referred to as the “blocking temperature” of the sample. For ZFC curves measured under increasing field amplitudes, the peak is expected to reflect the lowering of the anisotropy barriers, and hence should shift towards lower temperatures (as observed e.g. in [1]).

However, in several experiments [2, 3, 4, 5], an astonishing increase of the ZFC-peak temperature with the field amplitude has been reported. In the first papers [2, 3], no explanation was proposed for this apparent barrier increase under the effect of the applied field. In very recent works on antiferromagnetic particles of ferritin [4, 5], interestingly, the effect has been discussed as a possible indication of a resonant spin tunneling phenomenon [6]. In brief, if the magnetic moment of the particles can flip by quantum tunneling through the anisotropy barrier (a process which should be favored in antiferromagnetic particles [7]), then the flipping rate should be enhanced by a resonance effect when the up and down energy levels coincide. In Mn-12 magnetic molecules, where the energy levels can be well defined, the resonances have been recently observed for the corresponding values of the field [8, 9]. In a system of size-distributed particles, there can be no coincidence of the various up and down energy levels in the different particles, except in the symmetrical situation of zero field. Resonant tunneling has thus been suggested to produce an increase of the relaxation rate around zero field [6], which could (among other evidences, see [4, 5]) show up as the observed anomalous increase of the ZFC-peak temperature for increasing fields.

In the present paper, we want to address the question of the origin of this anomalous behavior, and to argue in favor of other characterization procedures than the ZFC measurement. We first present a series of experiments on a sample of $\gamma - Fe_2O_3$ particles, which do indeed exhibit the ZFC anomaly in the $\sim 65K$ region, a rather high temperature range for expecting evidences of quantum effects. Under some simple approximations, we discuss the expression of the ZFC magnetization, and point out that the peak temperature is strongly influenced by the width of the barrier distribution. We propose

as a possible explanation of the anomaly that this width increases under the influence of increasing field.

In comparison with the ZFC-peak results, we use another experimental procedure, which also gives access to a characteristic temperature depending on the applied field amplitude. This other characteristic temperature can be expected to be much less sensitive to the width of the barrier distribution (and even insensitive in an ideal log-normal case). Our measurements on $\gamma - Fe_2O_3$ particles indeed show that this characteristic temperature decreases for increasing fields, without any anomaly. We also extract from the measurements an approximate width of the barrier distribution, which we find to slightly increase with field; the effect has the correct order of magnitude for reproducing the observed ZFC-anomaly.

The largest part of the present paper (Sect. 3 and 4) is devoted to the $\gamma - Fe_2O_3$ sample, which we have studied in more details until now [10, 11, 12]. We use these results as an example for discussing the physical information which can be extracted from the various experimental procedures. Finally, in Sect. 5, we apply the same procedures to a ferritin sample. As in the $\gamma - Fe_2O_3$ case, the anomaly is found in the ZFC measurements (in agreement with the other works [3, 4, 5]), whereas it does not show up with the other procedure, making likely our “classical” explanation of the ZFC-anomaly.

2 Experimental procedure and samples

Our first sample consists in small ferrimagnetic particles of $\gamma - Fe_2O_3$ (maghemite), which have been embedded in a silica matrix obtained by a room temperature polymerization process [13]. Other samples of the same batch have recently been used for studying the features of the magnetic relaxation in the limit of very low temperatures [10, 11]. Here, the particles are diluted to the very low volume fraction of $f_v = 2 \cdot 10^{-4}$, in order to favor independent relaxation processes of the particles. In a saturated sample (all particle moments being aligned, which is far from our case), the corresponding dipolar field would be of order 1 *Oe*.

We could not directly observe the $\gamma - Fe_2O_3$ particles in the TEOS matrix. However, TEM imaging of the particles before their incorporation in silica has been made; Fig.1 displays the resulting diameter histogram, which can be tentatively fitted (as is usually done in the literature) to a log-normal

shape

$$f(d) = \frac{1}{\sqrt{2\pi} \sigma_d d} \exp\left(-\frac{\ln^2 \frac{d}{d_0}}{2 \sigma_d^2}\right) , \quad (1)$$

yielding $d_0 = 7 \text{ nm}$ and $\sigma_d = 0.3$.

We have performed the magnetization measurements with a commercial SQUID magnetometer (from Cryogenic Ltd, U.K.). Fig.2 presents example curves from the $\gamma - Fe_2O_3$ sample, obtained at a given field amplitude along various procedures. The ZFC curve is measured as explained above. The “FC” (Field Cooled) curve is obtained by cooling the sample in the field, and measuring while increasing the temperature. We have used in addition a less common measurement procedure, which we denote as “R-TRM” (Reversed Thermo-Remanent Magnetization); it consists in cooling the sample in the field, reversing the field at low temperature, and then measuring upon increasing the temperature. Compared to the more usual “TRM” procedure, in which the field is cut-off instead of being reversed, it presents the advantage that the field conditions for the initial and final states of the particle relaxation are identical; the effect of the field amplitude on the barrier distribution can be studied more directly, as we argue below.

Our second sample in this study is made of horse-spleen commercial ferritin (Sigma Chimie). Ferritin is an iron-storage protein; it consists in a protein shell of outer and inner diameters 12nm and 7.5nm , which is partially or completely filled with an antiferromagnetic iron oxide core (maximum of ~ 5000 Fe ions per ferritin molecule) [14]. The concentration of our solution is 100mg/ml , which again corresponds to a dipolar field of order 1Oe (at saturation of the non-compensated moments). As an example of antiferromagnetic nanoparticles, ferritin is considered a good candidate for the observation of quantum tunneling of the Néel vector [7], and has been the subject of numerous studies at low temperatures these last years (see [3, 4, 5, 15, 16] and references therein).

All throughout the paper, we have chosen as a convention to present the results in terms of magnetic moments, in conventional c.g.s. electromagnetic units; we have not divided the measured magnetic moments by the sample volume, which we estimate for the $\gamma - Fe_2O_3$ particles to $V_{tot} = 2.1 10^{-5} \text{ cm}^3$. For ferritin, we only know the total mass, which amounts to $8.4 10^{-3} \text{ g}$ of ferritin particles. Coherently, in the following equations, we do not divide by integrals over the particle volumes.

3 ZFC measurements: anomalous field dependence

We present now the ZFC measurements which we have performed on our sample of $\gamma - Fe_2O_3$ particles, for field amplitudes ranging from 1 to 200 Oe (in this sample, the effective coercive field which brings the magnetization to zero after saturation is ~ 300 Oe at 2 K [12]). The curves are displayed in Fig.3a, and the peak temperature variation with the field is shown in Fig.3b. Surprisingly, the peak temperature increases with the field up to ~ 80 Oe , before decreasing for larger values as expected.

The initial increase of a ZFC curve reflects the additive contributions of larger and larger particles which are deblocked as the temperature is raised; the maximum is obtained when these contributions are compensated by the superparamagnetic reduction of already deblocked moments. It is therefore clear that the peak temperature has no simple relation with the peak of the size distribution. One may however consider that it is related to some typical anisotropy barrier; in that case, the effect of an increasing field amplitude should be to lower the anisotropy barrier, in contradiction with our result in Fig.3b.

A similar observation has already been reported for magnetite particles [2], and also in ferritin [3]; no explanation was proposed. Again in ferritin, the phenomenon has recently been quoted [4, 5], and discussed as a possible indication of a resonant tunneling process at zero field [6]. In our present sample, the temperature range of the ZFC-peak (~ 65 K) does not favor an explanation of quantum origin. In the following, we write in more details the M_{ZFC} expression under simple assumptions, and propose a semi-quantitative explanation of a non-monotonic behavior of the peak temperature in terms of the field influence on the barrier distribution.

The ZFC data being taken in a field H , deblocking of particles with anisotropy barrier $U(H)$ occurs at a temperature T_b such that the typical time for crossing the barrier $U(H)$ is equal to the measurement time $t_m \sim 100$ s, namely

$$k_B T_b = \frac{U(H)}{\ln t_m / \tau_0} \quad (2)$$

where the attempt time τ_0 is of order 10^{-10} s, giving $\ln t_m / \tau_0 \simeq 28$. We assume that the anisotropy barrier U of a particle is proportional to its volume V ;

in zero field, $U = KV$, where K is the energy density for uniaxial anisotropy (from other measurements, $K \simeq 6 \cdot 10^5 \text{ erg/cm}^3$ [12]). In the general case of random orientations of the easy axes of the particles, the question of the field dependence $U(H)$ of the anisotropy barriers cannot be solved analytically (approximations are discussed in [17]). If the easy axes are parallel to the field, in contrast, it is straightforward to derive exactly

$$U(H) = KV\left(1 - \frac{H}{H_c}\right)^\alpha \quad (3)$$

with $\alpha = 2$. H_c is the coercive field, at which the given barrier vanishes. In [18], it has been observed that the disorder of the easy axes orientations yields a distribution of the H_c values. We restrict ourselves to simply considering that we can approximate the orientational disorder by Eq.3 with $\alpha = 1.5$ instead of $\alpha = 2$ [19], keeping the same H_c for all particles.

At a given temperature T , the magnetization M_{ZFC} is the sum of the superparamagnetic contributions of the particles for which $T_b < T$, or in other words of volume smaller than a blocking value V_b such that

$$V_b(T, H) = \frac{k_B T \ln t_m / \tau_0}{K(1 - H/H_c)^\alpha}. \quad (4)$$

For the sake of simplicity, we approximate here the superparamagnetic behavior by an $1/T$ Curie shape, and do not include a temperature dependence of the saturated magnetization M_s . We do not expect these approximations to significantly affect the present discussion (see more detailed analysis in [12]).

Within this framework, M_{ZFC} reads

$$M_{ZFC}(T) = M_r(H) + \frac{M_s^2}{3 k_B T} H \int_0^{V_b(T, H)} f(V) V^2 dV. \quad (5)$$

where M_r stands for the reversible contribution which is due to the canting of the moments from the easy axes towards the field direction. This term equals $M_r = M_s^2 V_{tot} H / 3 K$ in the $T = 0$ limit; at non-zero temperatures, it is a correction to the main term which accounts for the fact that the moments are not exactly lying along the easy axes. As is usually done, we neglect it in the present discussion of the ZFC-peak; we show below that this term disappears to first order in some other quantities.

Firstly, one sees in Eq. 5 that the temperature dependence of M_{ZFC} occurs (at least) via $V_b(T, H)$ and the Curie term. The temperature derivative

cannot be written in simple terms, and there is no explicit expression of the peak temperature (which, however, obeys a simple first-order differential equation [20]). Secondly, the $f(V)$ distribution is here involved through a $V^2 f(V)$ contribution, which clearly emphasizes the effect of the largest particles; the sensitivity of M_{ZFC} to the standard deviation $\sigma_v = 3\sigma_d$ is stronger than that of other quantities which involve lower powers of V , like the one that we propose below.

In order to quantitatively estimate the sensitivity of M_{ZFC} to σ_v , we have performed numerical calculations of Eq.5, which are shown in Fig.4a. The K and V_0 parameters have been adjusted to the values of the experiment; in this elementary calculation, due to the various approximations, the shape of the ZFC curves is not completely realistic [12]. However, one sees clearly in Fig.4a that the ZFC-peaks shifts extremely rapidly towards higher temperatures when σ_v is increased. In Fig.4b, we present the ratio of the ZFC-peak temperature to the blocking temperature for the typical volume V_0 . For our sample ($\sigma_v \sim 0.9$), the calculation yields a ratio of 4.4 (neglecting the $M_s(T)$ variation should produce a slight overestimate). In most cases found in the literature, the standard deviation of the volume distribution is of this same order of magnitude; the particle volume which is commonly deduced from the ZFC-peak must therefore be divided by a non-negligible factor before being compared with V_0 .

In our opinion, the result in Fig.4b opens the way to a possible explanation of the $T_b(H)$ increase at low fields, which could be due to a slight enlargement of the barrier distribution under the influence of the field. A simple reason for that can be the disorder of orientations. For randomly oriented particles of a unique size, the applied field lowers differently the barriers with respect to their orientation, thus enlarging the barrier distribution. Such an enlargement can indeed be found in our R-TRM data (see below).

4 Other measurement procedures for probing the barrier distribution

A TRM measurement corresponds to the inverse field-history of the ZFC procedure; the sample is cooled in the field, the field is cut at low temperature, and deblocking is measured for increasing temperatures in zero field. Keeping the same assumptions as above, the TRM can be written as the sum of the

moments which are still blocked in the field-cooled state:

$$M_{TRM}(T) = \frac{M_s^2}{3 k_B} H \int_{V_b(T,0)}^{\infty} \frac{f(V) V^2}{T_b(V, H)} dV . \quad (6)$$

Contrary to the ZFC case, no M_r term appears, and now the $1/T$ term is replaced by $1/T_b$, since each particle has kept a magnetization which is equal to the superparamagnetic value at the blocking temperature $T_b(V, H)$. T_b is obtained from Eqs. 2,3, where t_m now corresponds to the time scale τ_c of blocking during the field-cooling process. An estimate of τ_c can be obtained from the cooling rate $v_c = dT/dt$ ($\simeq 0.04 K/s$). As the temperature decreases, the Arrhenius relaxation time τ for a given barrier abruptly increases, and freezing occurs when $\partial\tau(t)/\partial t \sim 1$. One finds that τ_c satisfies

$$\tau_c \ln^2 \frac{\tau_c}{\tau_0} = - \frac{U}{k_B v_c} , \quad (7)$$

which yields $\tau_c \sim 30 s \sim t_m$ for $U = KV_0$; the $\ln t_m/\tau_0$ term which is involved in T_b for the TRM procedure is almost the same as above. Replacing now $T_b(V, H)$ in Eq.6, we obtain:

$$M_{TRM}(T) = \frac{M_s^2 \ln t_m/\tau_0}{3K(1 - H/H_c)^\alpha} H \int_{V_b(T,0)}^{\infty} f(V) V dV . \quad (8)$$

The only temperature dependence of the TRM occurs in the lower bound $V_b(T, 0)$ of the integral; this allows us to take very simply the temperature derivative of M_{TRM} [21], which reads

$$\frac{\partial M_{TRM}}{\partial T} = - \frac{M_s^2 k_B H}{3 K^2} \frac{\ln^2 t_m/\tau_0}{(1 - H/H_c)^\alpha} V_b(T, 0) f(V_b(T, 0)) . \quad (9)$$

Thus, the TRM derivative gives a direct access to the quantity $Vf(V)$; if $f(V)$ is log-normal, then $Vf(V)$ peaks at $V = V_0$, independently of the width of the distribution. This makes a crucial difference with the ZFC case, for which the peak rapidly shifts as σ_v increases. However, the blocking volume $V_b(T, 0)$ which is involved in $\partial M_{TRM}/\partial T$ is the blocking volume in zero field, because the measurement is performed in zero field. The effect of the field amplitude only appears through a multiplicative factor in Eq.9; in other words, $\partial M_{TRM}/\partial T$ does not give access to the field-modulated barrier distribution.

This is our motivation for proposing the use of another experimental procedure, which allows the study of the effect of the field amplitude on the barrier distribution. We have performed a series of “Reversed-TRM” measurements (R-TRM) for various field values; after field-cooling in $+H$, the field is reversed to $-H$ at low temperature, and the magnetization is measured while increasing the temperature. An example of such a curve has been given in Fig.2. Within the same framework as above, the magnetization M_{R-TRM} at a given temperature T can be written as the sum of the contributions of the smaller particles, already deblocked at T in $-H$, plus that of the larger ones, still blocked in the $+H$ field-cooled state; again using the $T_b(V, H)$ expression for the blocked term, one obtains

$$M_{R-TRM}(T, H) = M_r(-H) + \frac{M_s^2 H}{3} \left[-\frac{1}{k_B T} \int_0^{V_b(T, H)} f(V) V^2 dV + \frac{\ln(t_m/\tau_0)}{K(1 - H/H_c)^\alpha} \int_{V_b(T, H)}^\infty f(V) V dV \right]. \quad (10)$$

This expression looks rather complicated; but it is almost the same as that of the field-cooled magnetization M_{FC} , up to the respective signs of the superparamagnetic contributions (also, the reversible parts M_r are just of opposite sign). In a $+H$ field, M_{FC} reads:

$$M_{FC}(T, H) = M_r(+H) + \frac{M_s^2 H}{3} \left[\frac{1}{k_B T} \int_0^{V_b(T, H)} f(V) V^2 dV + \frac{\ln(t_m/\tau_0)}{K(1 - H/H_c)^\alpha} \int_{V_b(T, H)}^\infty f(V) V dV \right]. \quad (11)$$

The idea is to consider the sum $M_{R-TRM} + M_{FC}$ of both magnetizations, and thus get rid of the superparamagnetic contribution (and of M_r), which presents the most intricate temperature dependence:

$$M_{R-TRM}(T, H) + M_{FC}(T, H) = 2 \frac{M_s^2 H}{3} \frac{\ln(t_m/\tau_0)}{K(1 - H/H_c)^\alpha} \int_0^{V_c(T, H)} f(V) V dV. \quad (12)$$

As in the TRM case (Eqs. 6,8), the temperature derivative can easily be taken:

$$\frac{\partial(M_{R-TRM} + M_{FC})}{\partial T} = -2 \frac{M_s^2 H k_B \ln^2 t_m/\tau_0}{3K^2(1 - H/H_c)^{2\alpha}} V_b(T, H) f(V_b(T, H)). \quad (13)$$

In this quantity, the blocking volume corresponds to blocking in a field H , a quantity which was not involved in simple TRM measurements. Using our R-TRM and FC measurements, we have estimated the derivatives Eq.13 for our $1 - 200$ Oe measurement fields; the resulting curves are displayed in Fig.5a. If the $f(V)$ distribution is log-normal, then $Vf(V)$ is a simple gaussian of $\ln V/V_0$, which peaks at V_0 whatever the distribution width. One may therefore argue that the peak of this quantity in different fields corresponds to the same objects. Obviously, the assumption of a log-normal $f(V)$ remains questionable (see below); however, within this assumption which is the most commonly used, our procedure allows a clearly more direct characterization of the barrier distribution than the ZFC measurement.

The peak temperatures of Fig.5a are plotted versus H in Fig.5b, which can be compared with the ZFC data in Fig.3b. The peak temperatures monotonically decrease with increasing field, whereas the ZFC results were exhibiting a striking non-monotonic behavior. The peak temperatures can be fitted to the expected field-dependence Eq.3; fixing $\alpha = 1.5$ [19] and $V_0 = 180$ nm^3 from TEM (Fig.1), we obtain $H_c \simeq 250$ Oe and $K = 6.4 \cdot 10^5$ erg/cm^3 , in good agreement with other estimates [12].

Another combination of R-TRM and FC data can be used for checking the overall coherence of our data and analysis. According to Eqs. 5,10 and 11, the three kinds of experiments are related:

$$M_{ZFC} = \frac{1}{2}(M_{FC} - M_{R-TRM}) , \quad (14)$$

or, in other words, given two of the measurements, the third one can be deduced. This is what we have made in the ZFC case; Fig.6a compares the measured ZFC magnetizations (symbols) with the ones which are obtained by combining FC and R-TRM through Eq.14. They are in rather good agreement, except a slight amplitude difference in the vicinity of the peak for the lower field curves. In Fig.6b, we compare the field variation of the ZFC-peaks obtained in both direct and indirect way; they are fully compatible within the errors bars, and in particular the non-monotonic behavior is found in both cases, whereas it does not show up in the FC+R-TRM analysis of Fig.5b.

The fact that the anomalous behavior of the ZFC-peak does not appear in a (FC+R-TRM) measurement, which is less sensitive to the $f(V)$ width, prompts us to propose that the initial increase of the ZFC-peak with increasing field be related to an increase of the distribution width. This effect can

be searched in the $V_b f(V_b)$ data which were presented in Fig.5a; in Fig.7, we present differently this same data, in a way which favors the comparison of the various curves. If $f(V_b)$ is log-normal, all $V_b f(V_b)$ curves are simple gaussians of $\ln T$; their peak temperature corresponds to blocking V_0 in a field H , that is the peak temperatures are deduced from each other by a multiplicative factor (which is the effect of the field on the anisotropy barrier). In Fig.7, the data is presented as a function of $\ln T$, and the peaks are superposed by a T-affinity; also, for clarity, the peak amplitudes have been normalized to one.

A slight but systematic asymmetry of the curves can be noted; they are a little bit more spread out on the low-T side. The derivative estimate of the first points can be less accurate; apart from that difficulty, the effect suggests that the log-normal approximation is not completely correct. This may indicate a difference between the geometrical sizes which are seen by TEM and the effective magnetic sizes. However, the accuracy with which the size histogram of Fig.1 suggests a log-normal shape is less than that of Fig.7. The universal success of the log-normal shape for particle size distributions could be more related to practical reasons than really scientifically grounded.

Even slightly asymmetric, the curves in Fig.7 show that the width of the effective distribution increases for increasing field. Within the present assumptions, we do not intend to reproduce in details the observed ZFC-peak temperature variation, but we can roughly quantify the effect. For example, when H goes from 1 to 50 Oe, the approximative σ_v which can be read in Fig.7 increases from 0.8 to 1.1. For $H_c = 250$ Oe as obtained above, and using Eq.3 with $\alpha = 1.5$ for the field influence on the barriers, we have computed the corresponding ZFC curves; the curve with $(H = 50$ Oe, $\sigma = 1.1)$ peaks at a 1.3 times higher temperature than the one with $(H = 1$ Oe, $\sigma = 0.8)$. Hence, for increasing field, the observed distribution enlargement is enough for producing an increase of the ZFC-peak temperature, despite the lowering of the barriers.

5 Ferritin results

In ferritin, a non-monotonic variation of the ZFC-peak, together with other particular features of the magnetization relaxation, has been discussed in terms of resonant tunneling at zero field [4, 5]. A “pinch” of the hysteresis loop is observed around $H = 0$ [4, 5]; viscosity data can be interpreted as

showing an anomaly [5] (not yet clear in [4]), but this latter point still raises the question of a relevant normalization for the comparison of viscosity data at various fields, which is not yet completely solved [4],[22]. The observation of resonant tunneling is more plausible in ferritin than in the $\gamma - Fe_2O_3$ particles, because of the antiferromagnetic character of the particles, which makes their resultant moment smaller (~ 50 iron moments); the energy level spacing is thus larger, making wider the field range around zero where the effect can be visible [6]. Prompted by discussions with some of the authors of [4] and [5], we have measured a commercial ferritin sample and applied the same analysis as above for $\gamma - Fe_2O_3$ particles.

We have performed the measurements for fields ranging from 50 to 6000 Oe. The ZFC curves are shown in Fig.8a, together with the field dependence of the peaks in Fig.8b. Here again a non-monotonic variation is found, in agreement with previous works [3, 4, 5]. Following the procedure of Sect.4, we have also measured the FC and R-TRM curves at the same fields, and estimated the temperature derivative of the sum, which is shown in Fig.9a (peak values in Fig.9b). The result is qualitatively similar to the case of the $\gamma - Fe_2O_3$ particles. A slight tendency to increase can be seen in Fig.9b on the three points below 1000Oe, but it remains far smaller than the error bars; more accurate data would be needed for discussing this point. In the region of a few thousands of Oe where the ZFC-peak data show a clear maximum, the peak values of the derivative monotonically decrease for increasing field. Thus, on both samples that we have studied, the same apparently anomalous behavior is obtained from ZFC curves, and the anomaly is not confirmed in the other procedure. The analysis of $\partial(M_{FC} + M_{R-TRM})/\partial T$ seems therefore able to provide a physical information which is of much more direct interpretation than that extracted from ZFC measurements.

6 Conclusions

In this paper, we have discussed the physical interpretation of standard magnetic measurement procedures in systems of nanometric magnetic particles, on the basis of experiments performed with two very different samples. One is made of ferrimagnetic particles ($\gamma - Fe_2O_3$), highly diluted, with a ZFC-peak temperature of $\sim 65K$, and the other of antiferromagnetic particles of ferritin, less diluted but with much lower magnetic moment, with a ZFC peak in the $10 - 15K$ range.

In both samples, the ZFC-peak temperature is found to initially increase with field, at variance with the common sense expectation of an anisotropy barrier lowering due to the field. From a very simple description of the blocking and deblocking processes, we recall that the ZFC-peak temperature is not simply related to the typical volume of the distribution $f(V)$; it is influenced by the $1/T$ behavior of the deblocked particles, and involves a $V^2 f(V)$ term which enhances the contribution of the larger volumes. The ZFC curve is thus extremely sensitive to the distribution width; the peak rapidly shifts to higher temperatures when the width increases, an effect that we have quantified under simple approximations.

We propose to understand the ZFC anomaly at the light of another experimental procedure. As a first example, the temperature variation of the TRM, which is measured in zero field, does not involve the $1/T$ superparamagnetic contribution, and contains a $V f(V)$ term which yields a weaker sensitivity to the distribution width. But the TRM does not bring informations about the effective distribution of anisotropy barriers in a field. This point can be studied using a Reversed-TRM procedure, in which the field is reversed to its opposite value at low temperature. In the sum of the FC magnetization and the R-TRM, the $1/T$ term is eliminated (together with the reversible magnetization), and $f(V)$ comes in through $V f(V)$ (weak sensitivity to the width), in which V now stands for the volume which is deblocked in the field, thence the access to the field-modulated barrier distribution.

The temperature derivative $\partial(M_{FC} + M_{R-TRM})/\partial T$ of this sum is proportional to $V f(V)$, which peaks to a typical volume in the distribution, and our point is the following: for different experiments with various field amplitudes, the magnetic objects which correspond to the peak value remain almost the same (exactly the same in the log-normal case), which is far from being the case for ZFC measurements. Indeed, our measurements on both samples show that the peak of $\partial(M_{FC} + M_{R-TRM})/\partial T$ decreases for increasing field, in contrast with the peak of the ZFC curves.

The effect of the field on the distribution of anisotropy barriers is not easily described in details [17], mainly for two reasons. On the one hand, for random orientations of the particle easy axes, there is no general analytical treatment of the problem. On the other hand, the usual assumptions which are commonly made for describing systems of small particles might become less applicable in the presence of higher fields (is each particle a single fixed macro-moment, or will some weakly coupled parts align with the field ? are the particles relaxing independently, or do they become influ-

enced by the field of their neighbors ?). On the $\gamma - Fe_2O_3$ sample, which we have studied in more details than the ferritin, the examination of the measured $\partial(M_{FC} + M_{R-TRM})/\partial T$ shows that, for increasing field, $Vf(V)$ naturally peaks to lower values, but also becomes wider, as already expected from the only effect of orientational disorder. The effect has the correct order of magnitude for compensating the barrier decrease at low fields, and hence for producing the observed anomalous increase of the ZFC peak temperature. We therefore consider that the non-monotonic variation of the ZFC-peak temperature is related to an enlargement of the effective barrier distribution under the influence of the field; no anomaly is found using the other procedure.

There has been these last years a renewed interest for the low-temperature dynamics of systems of small particles, motivated by a search for quantum tunneling phenomena in these quasi-macroscopic objects [7]. Evidencing the quantum effects from viscosity measurements is hindered by the lack of knowledge of the effective barrier distribution, which modulates the temperature variation of the measured relaxation rates [10, 18]. Very recently, observations of the non-monotonic field dependence of the ZFC-peak temperature in ferritin [4, 5] have been discussed in terms of possible resonant tunneling effects in zero field [6]. This has prompted us to extend the present work, mainly centered on $\gamma - Fe_2O_3$ particles, to a ferritin sample. It appears that the same “classical” explanation of the ZFC anomaly should work in both cases. This conclusion does not concern other possible evidences of the resonant tunneling effects in ferritin, like e.g. the astonishingly pinched hysteresis cycles [4, 5]. Here again, as is the case for viscosity, it appears that the barrier distribution plays a non-negligible role, and that the choice of physically meaningful quantities for characterizing the low-temperature dynamics of magnetic nanoparticle systems remains a delicate matter.

We want to thank E.M. Chudnovsky for numerous stimulating discussions all along this work.

References

- [1] J. Tejada, X.X. Zhang and J.M. Hernandez, to be published in the Proceedings of *Magnetic Hysteresis in Novel Magnetic Materials* (Greece 1996), Editor H.J. Hadjipanayis, Kluwer Academic Publishers.
- [2] W. Luo, S.R. Nagel, T.F. Rosenbaum and R.E. Rosensweig, *Phys. Rev. Lett.* **67** (1991) 2721.
- [3] S. Gider, D.D. Awschalom, T. Douglas, K. Wong, S. Mann and G. Cain, *J. Appl. Phys.* **79** (1996) 5324.
- [4] J.R. Friedman, U. Voskoboinik, J. Li, M. Gunner and M.P. Sarachik, preprint 1997.
- [5] J. Tejada, X.X. Zhang, E. del Barco and E.M. Chudnovsky, preprint 1997.
- [6] E.M. Chudnovsky, preprint 1997.
- [7] B. Barbara and E.M. Chudnovsky, *Physics Letters A* **145** (1990) 205.
- [8] J.R. Friedman, M.P. Sarachik, J. Tejada, R. Ziolo, *Phys. Rev. Lett.* **76** (1996) 3830.
- [9] L. Thomas, F. Lioni, R. Ballou, D. Gatteschi, R. Sessoli and B. Barbara, *Nature* **383** (1996) 145.
- [10] R. Sappey, E. Vincent, M. Ocio, J. Hammann, F. Chaput, J.P. Boilot and D. Zins, *Europhys. Lett.* **37** (1997) 639.
- [11] R. Sappey, E. Vincent, M. Ocio and J. Hammann, submitted for the Proceedings of ICM 1997, cond-mat/9703248.
- [12] R. Sappey, PhD thesis (Université de Paris XI Orsay, France), in progress.
- [13] F. Chaput, J.-P. Boilot, M. Canva, A. Brun, R. Perzynski and D. Zins, *J. of Non-Cryst. Sol.* **160** (1993) 177; C.J. Brincker and G.W. Scherer, in “Sol-Gel Science”, Academic Press, New-York 1990.
- [14] G.H. Haggis, *J. Mol. Biol.* **14** (1965) 598; P.M. Harrison, F.A. Fischbach, T.G. Hoy and G.H. Haggis, *Nature* **216** (1967) 1188.

- [15] D.D. Awschalom, J.F. Smyth, G. Grinstein, D.P. DiVincenzo ahd D. Loss, *Phys.Rev. Lett.* **68** (1992) 3092.
- [16] J. Tejada and X.X. Zhang, *J. Phys.: Cond. Mat.* **6** (1994) 263.
- [17] J.L. Dormann, D. Fiorani and M. El Yamani, *Phys. Lett. A* **120** (1987) 95.
- [18] B. Barbara, L.C. Sampaio, A. Marchand, O. Kubo and H. Takeuchi, *J.M.M.M.* **136** (1994) 183.
- [19] R.H. Victora, *Phys. Rev. Lett.* **63** (1989) 457.
- [20] E.M. Chudnovsky and J. Tejada, *in* “Quantum Magnetic Relaxation”, in press.
- [21] M. El-Hilo, K. O’Grady and R.W. Chantrell, *J.M.M.M.* **114** (1992) 295.
- [22] Ll. Balcells, O. Iglesias and A. Labarta, preprint 1997, cond-mat/9704042.

Figure captions

Figure 1: Histogram of the $\gamma - Fe_2O_3$ particle diameters, as observed in TEM imaging (symbols). 454 particles have been sampled. The dotted line is a fit to a log-normal distribution, with $d_0 = 7.05nm$ and $\sigma_d = 0.32$.

Figure 2: Example magnetization curves from the $\gamma - Fe_2O_3$ particles ($H = 80Oe$), obtained following the different experimental procedures: Field-Cooled, Zero-Field Cooled, and Reversed Thermo-Remanent Magnetization (the R-TRM curve has been multiplied by -1 in the figure).

Figure 3a: Measured ZFC magnetizations on the $\gamma - Fe_2O_3$ sample, normalized to the field amplitude. From top to bottom, the field values are 1, 10, 20, 50, 80, 110, 150 and 200 Oe.

Figure 3b: Peak temperatures of the measured ZFC magnetization curves for $\gamma - Fe_2O_3$.

Figure 4a: Calculated ZFC curves, using a log-normal volume distribution, for various values of the standard deviation σ_v .

Figure 4b: Ratio of the calculated ZFC-peak temperatures to the blocking temperature corresponding to V_0 (reference volume of the log-normal distribution), for different values of the standard deviation σ_v .

Figure 5a: Temperature derivative of the sum of the measured magnetizations $M_{FC} + M_{R-TRM}$, divided by the field amplitude, for different fields ($\gamma - Fe_2O_3$ sample).

Figure 5b: Peak temperatures of the curves in Fig.5a, for different fields; these temperatures do not show the non-monotonic behavior which is found using the ZFC-peaks.

Figure 6a: Comparison for the $\gamma - Fe_2O_3$ sample of the measured ZFC magnetizations (symbols) with the combination of measured magnetizations $(M_{FC} - M_{R_{TRM}})/2$ (solid lines), showing the consistency of the data and of our description (the magnetizations are normalized to the field amplitude). The field values are the same as in Fig.3a.

Figure 6b: Comparison of the peak temperatures of the measured ZFC curves (full squares) with the peak temperatures of the combination $(M_{FC} - M_{R_{TRM}})/2$ of other measured magnetizations (open circles).

Figure 7: Temperature derivative (normalized to the peak amplitude) of the combination $(M_{FC} + M_{R-TRM})$ of measured magnetizations, as a function of the neperian logarithm of the temperature (normalized to the peak position), for the $\gamma - Fe_2O_3$ sample.

Figure 8a: Measured ZFC magnetizations on the ferritin sample, normalized to the field amplitude. From top to bottom, the field values are 50, 200, 600, 1000, 2000, 3000, 4500 and 6000 Oe.

Figure 8b: Peak temperatures of the measured ZFC magnetization curves for ferritin.

Figure 9a: Temperature derivative of the sum of the measured magnetizations $M_{FC} + M_{R-TRM}$, divided by the field amplitude, for different fields (ferritin sample).

Figure 9b: Peak temperatures of the curves in Fig.9a (ferritin sample), for different fields, which do not confirm the non-monotonic behavior observed for the ZFC-peak.

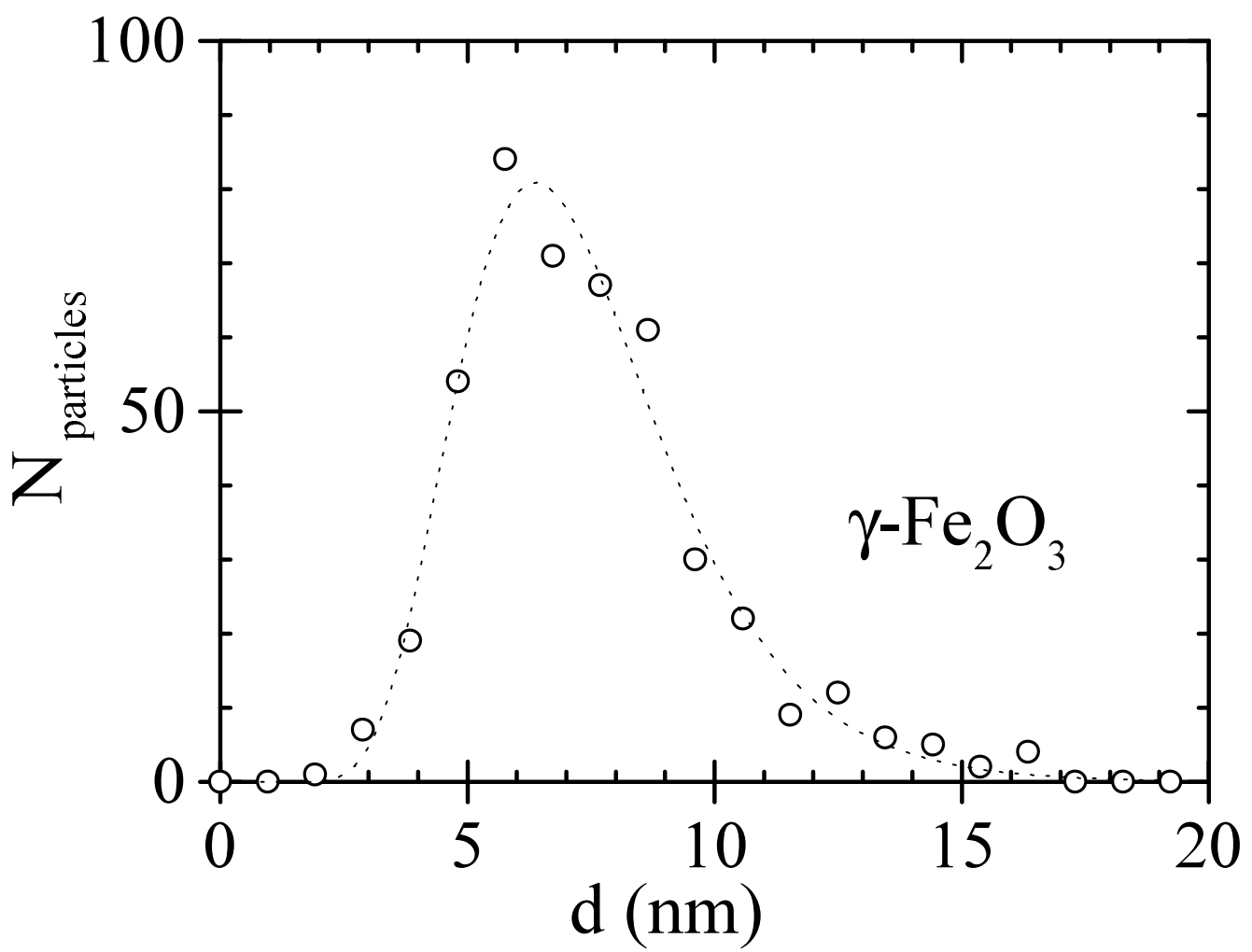


Fig. 1

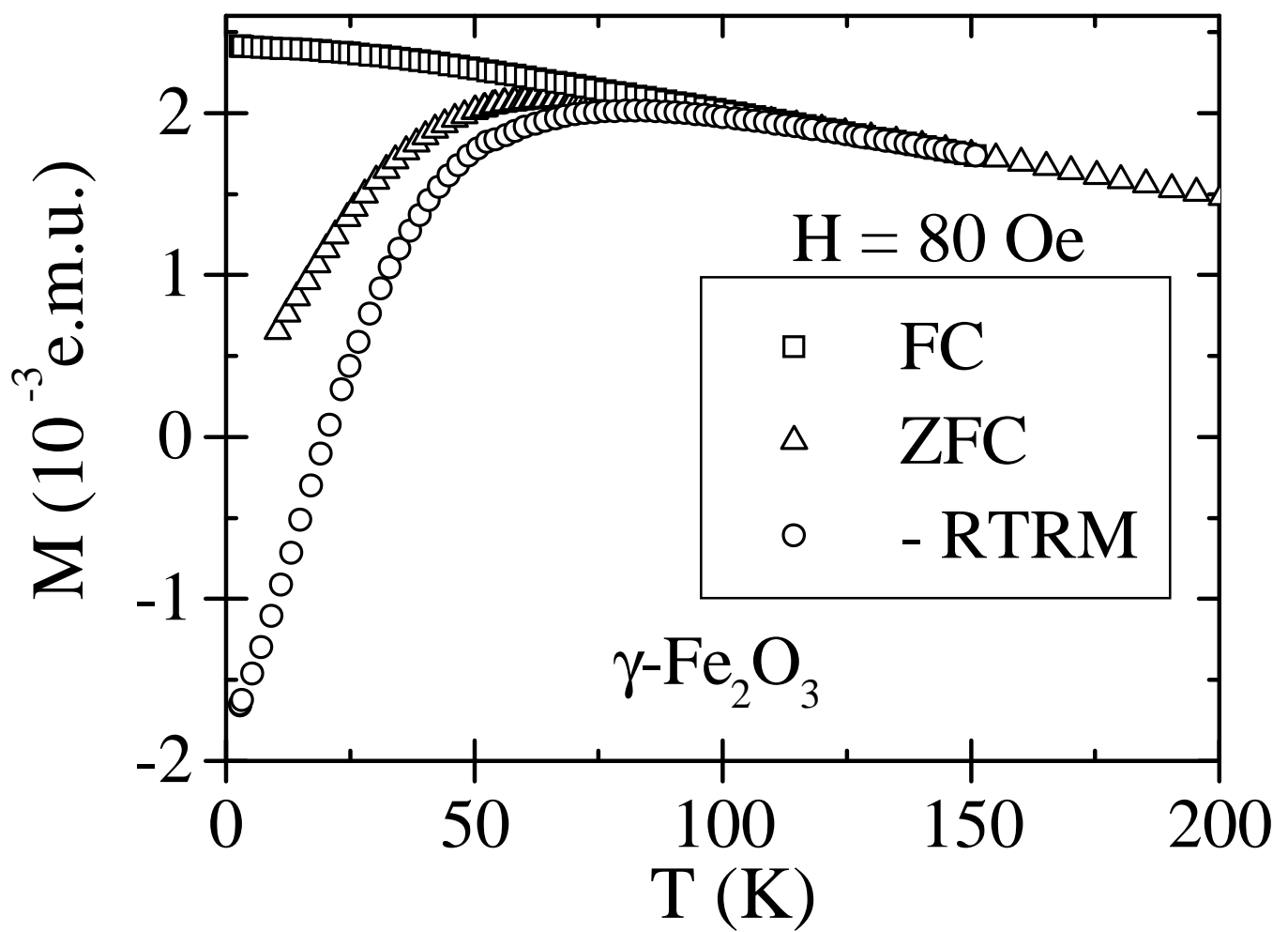


Fig.2

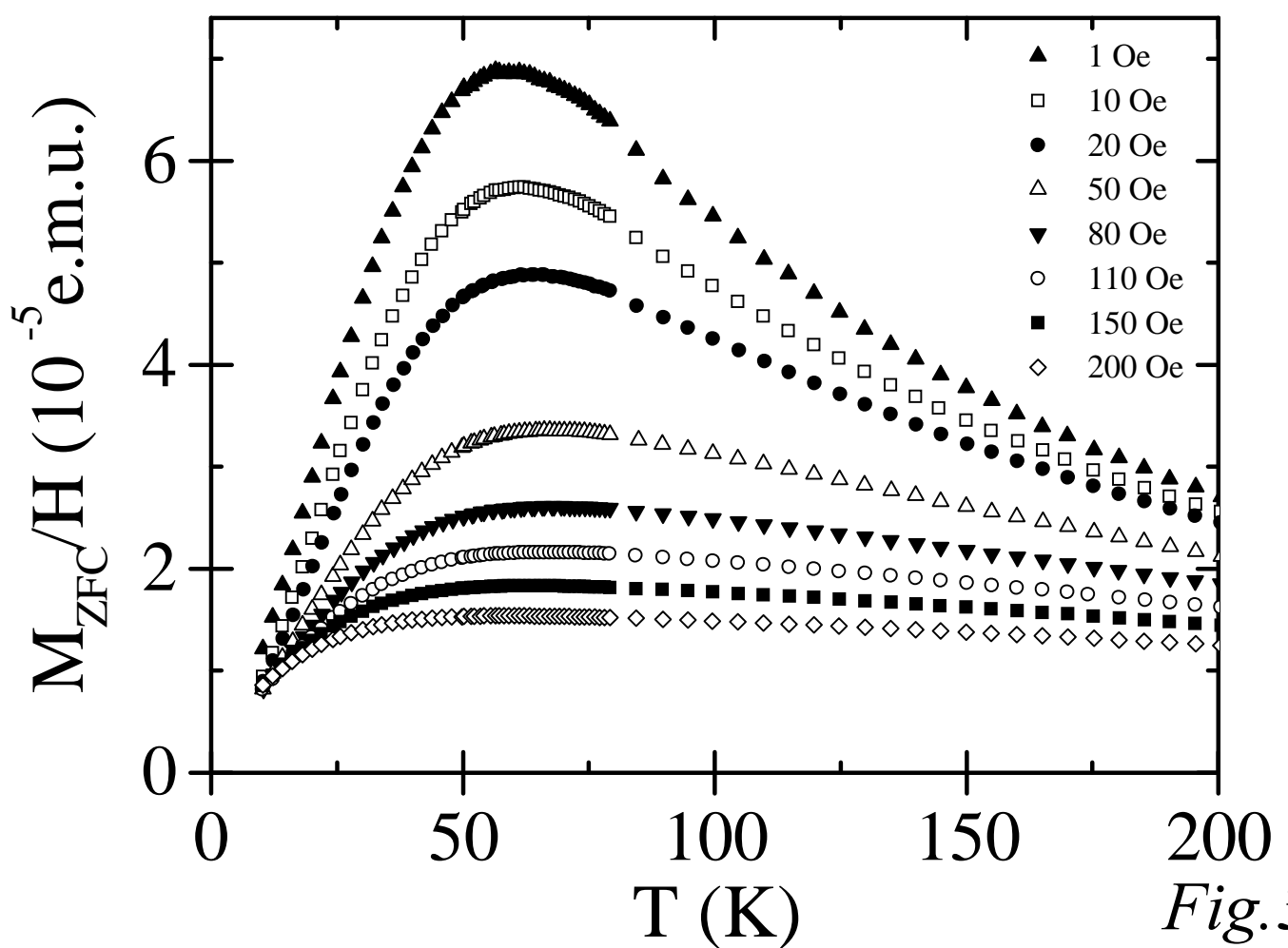
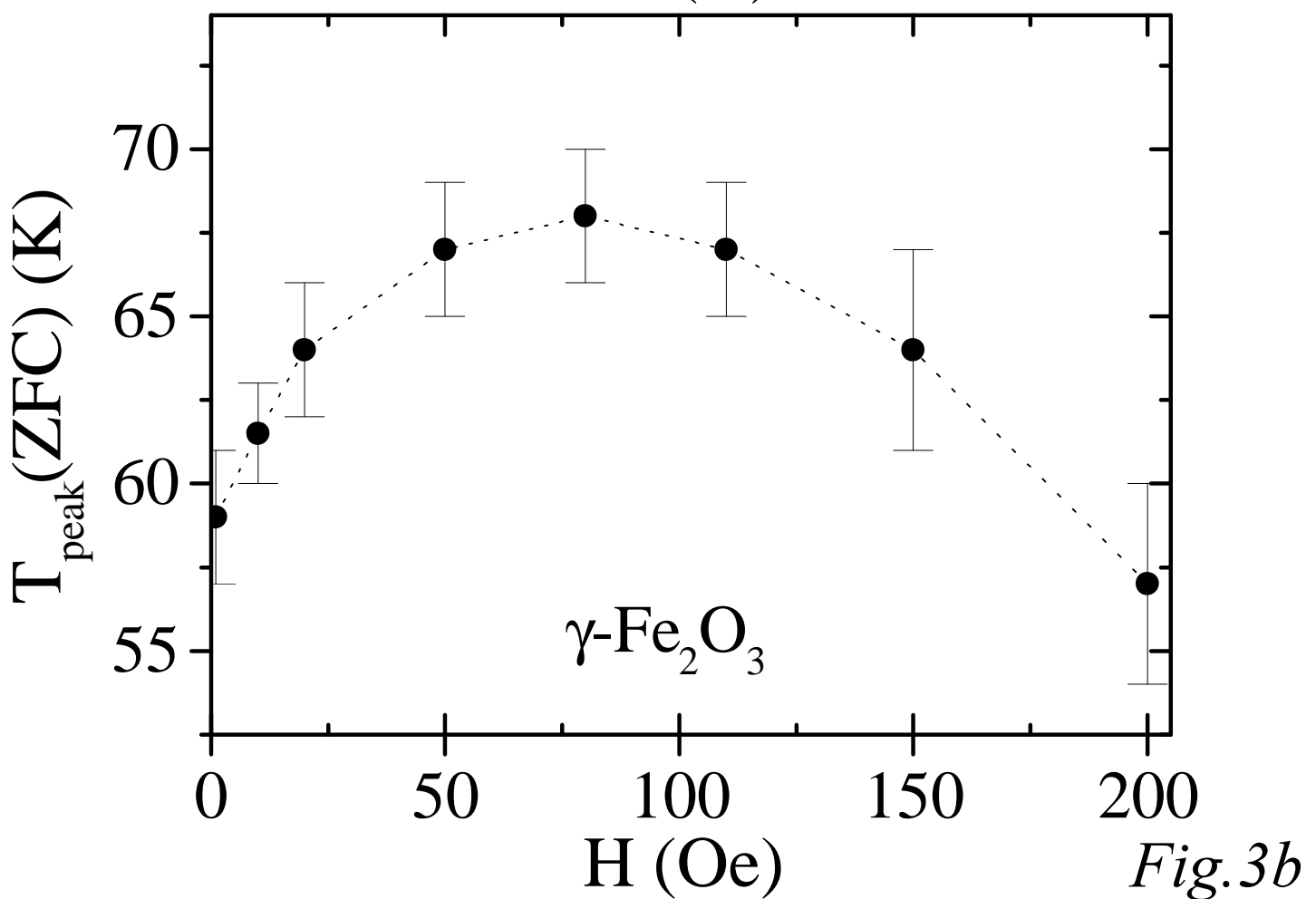


Fig. 3a



$\gamma\text{-Fe}_2\text{O}_3$

Fig. 3b

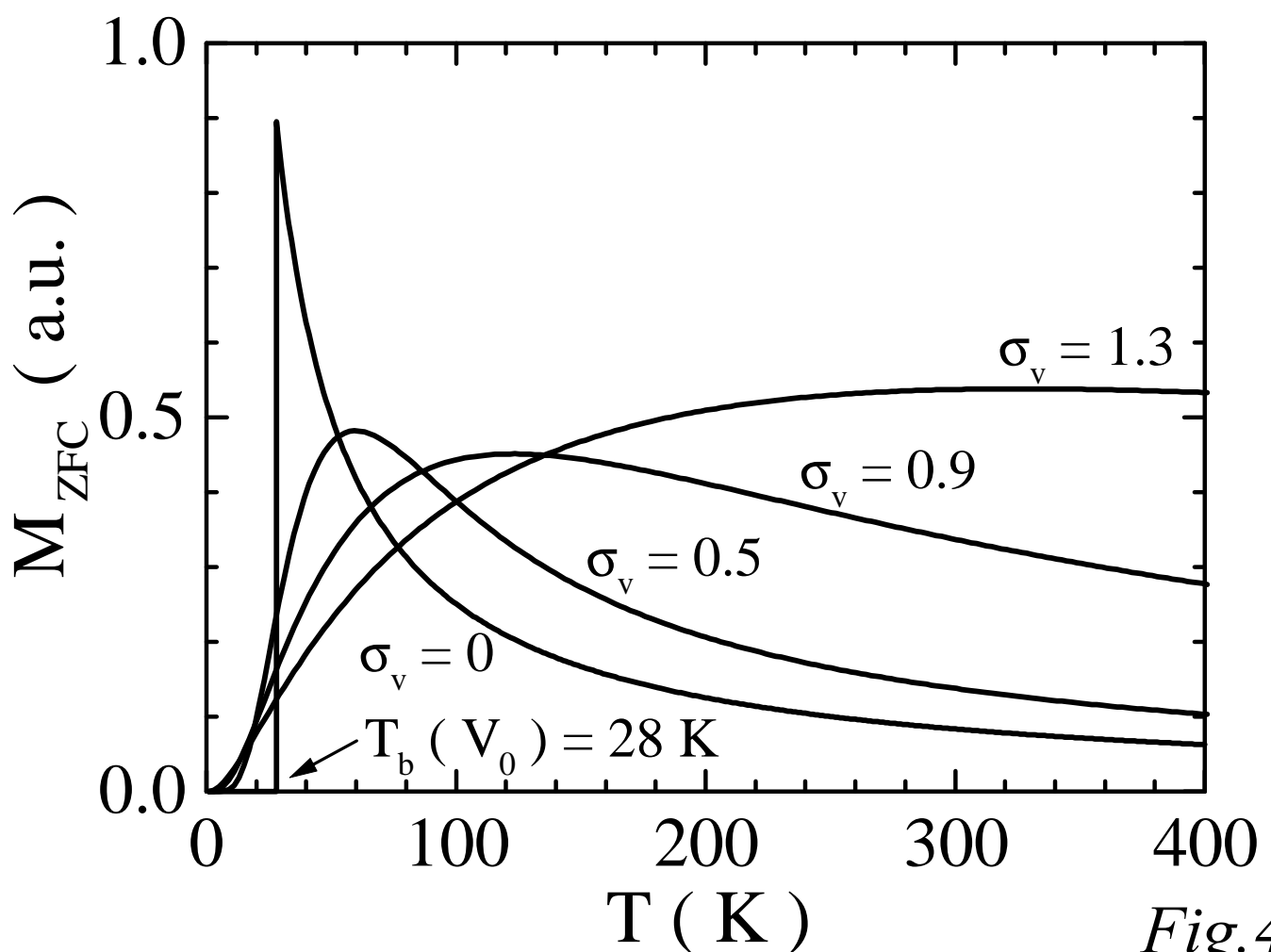


Fig.4a

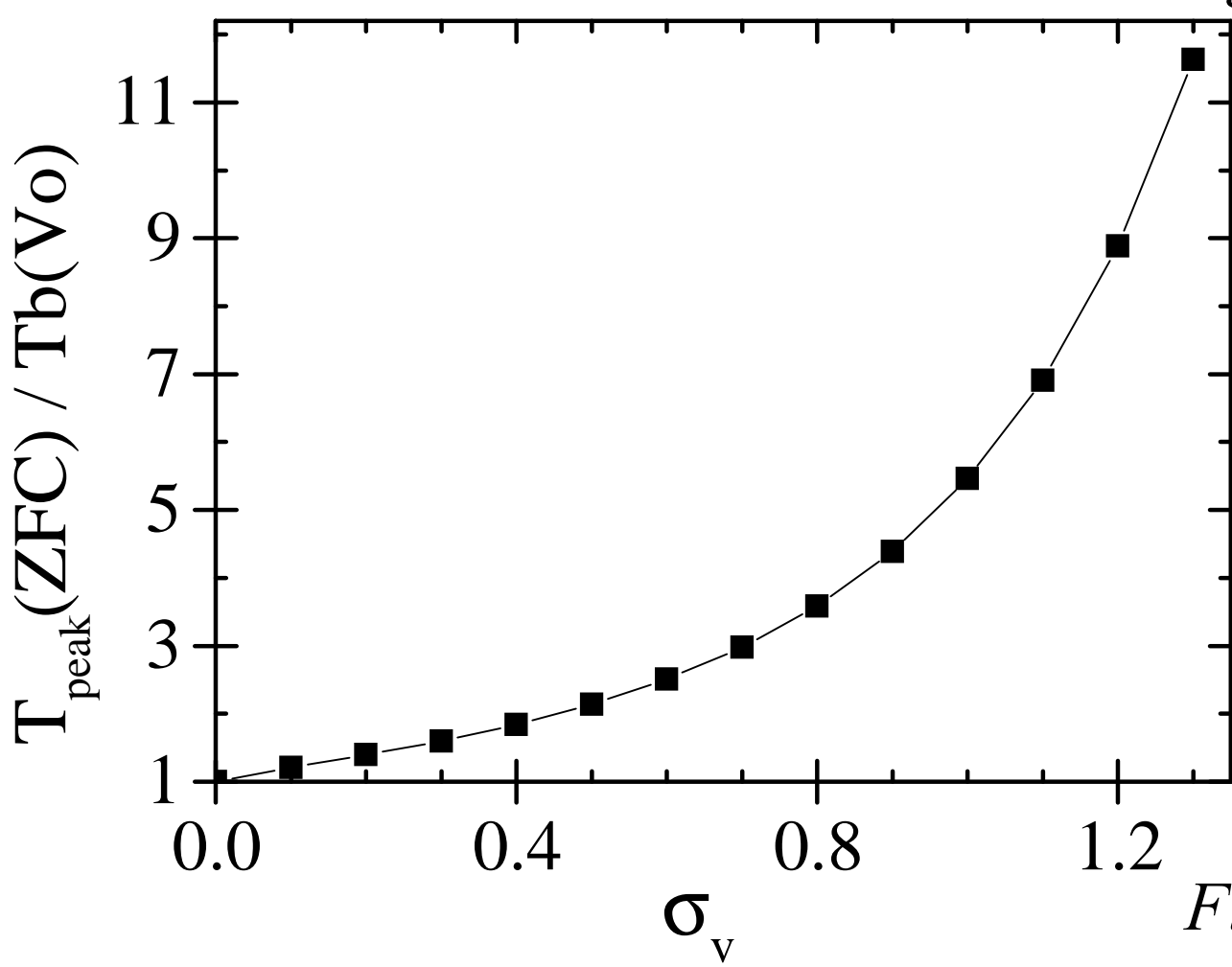


Fig.4b

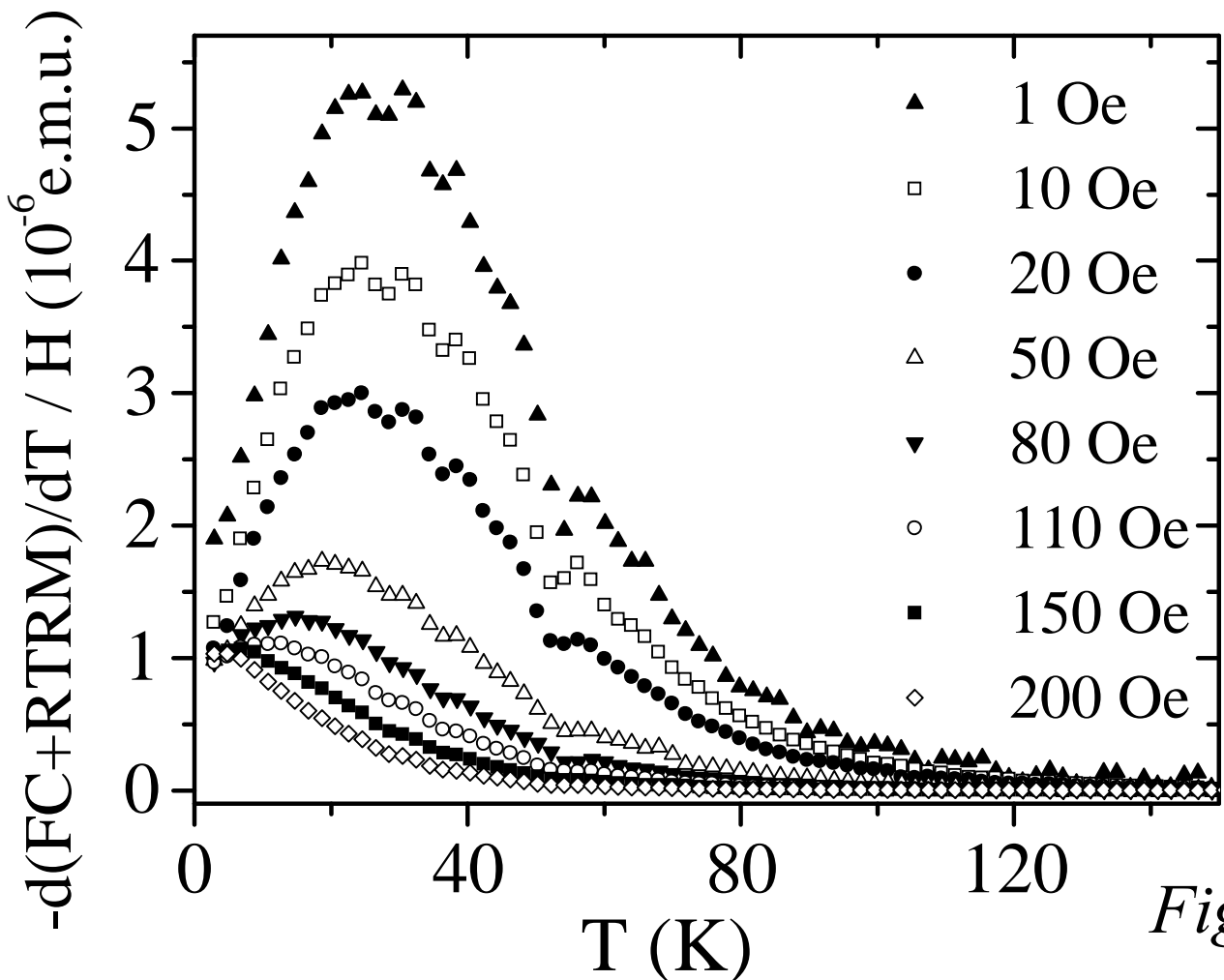
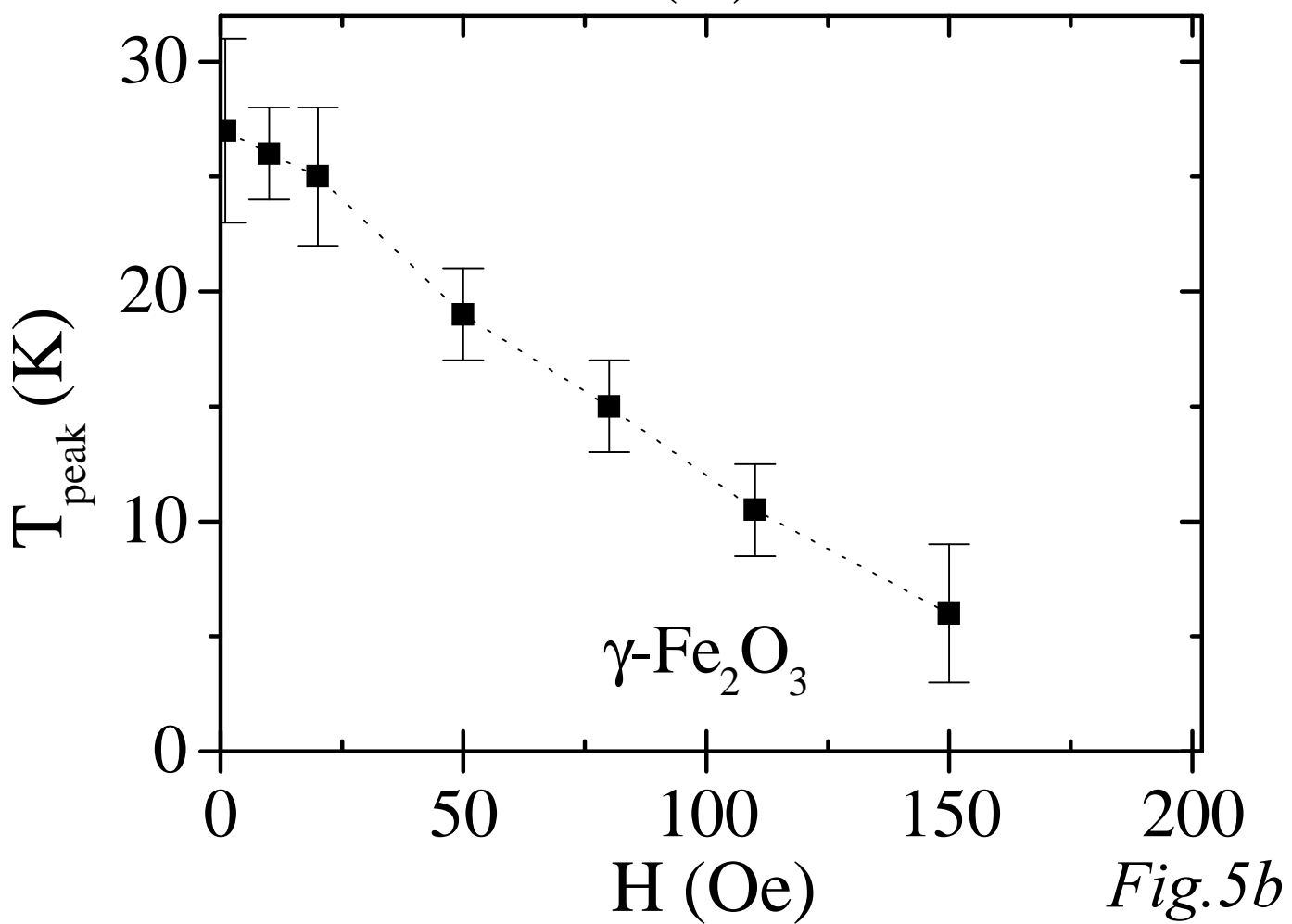


Fig. 5a



$\gamma\text{-Fe}_2\text{O}_3$

Fig. 5b

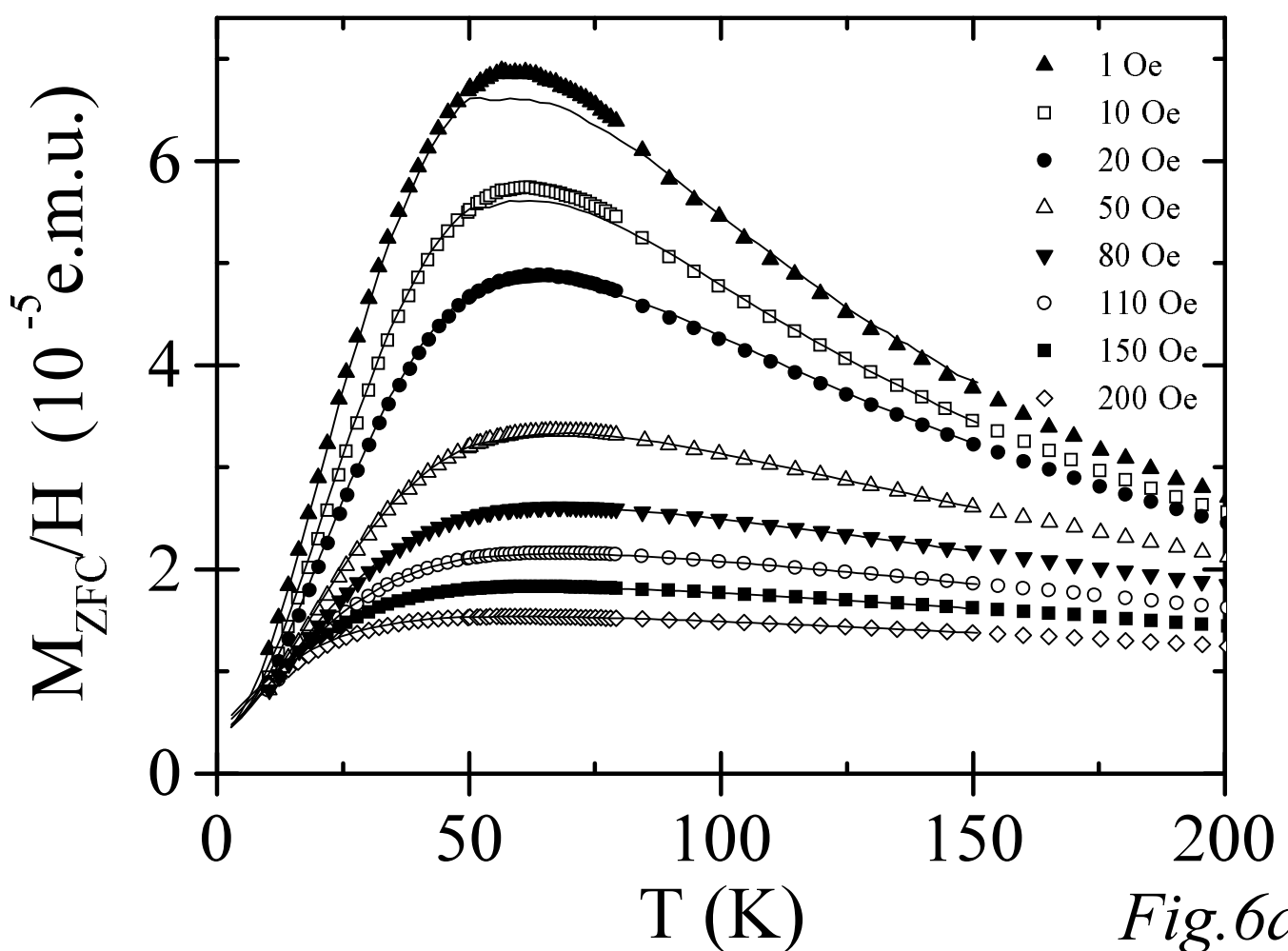
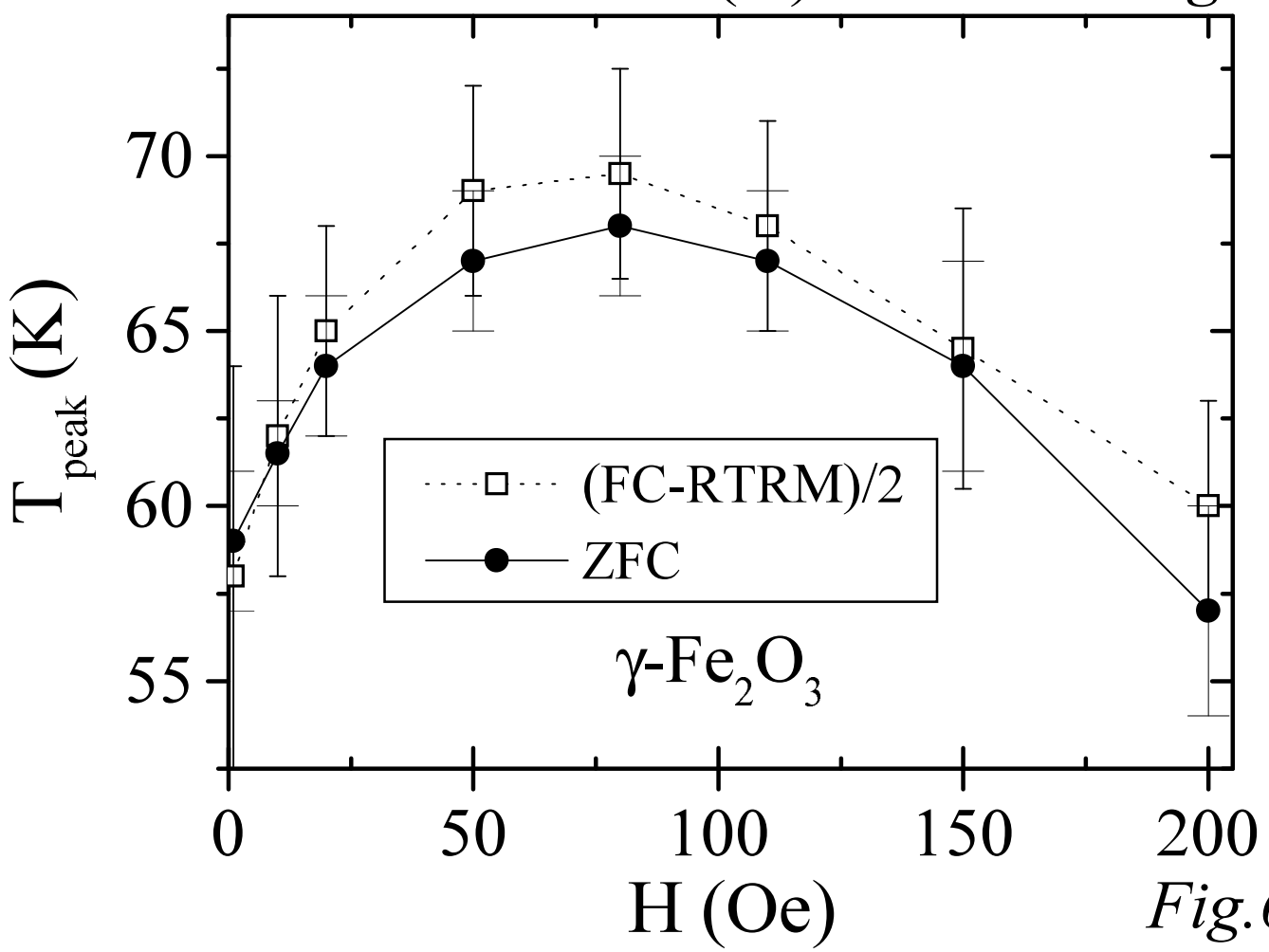


Fig.6a



$\gamma\text{-Fe}_2\text{O}_3$

Fig.6b

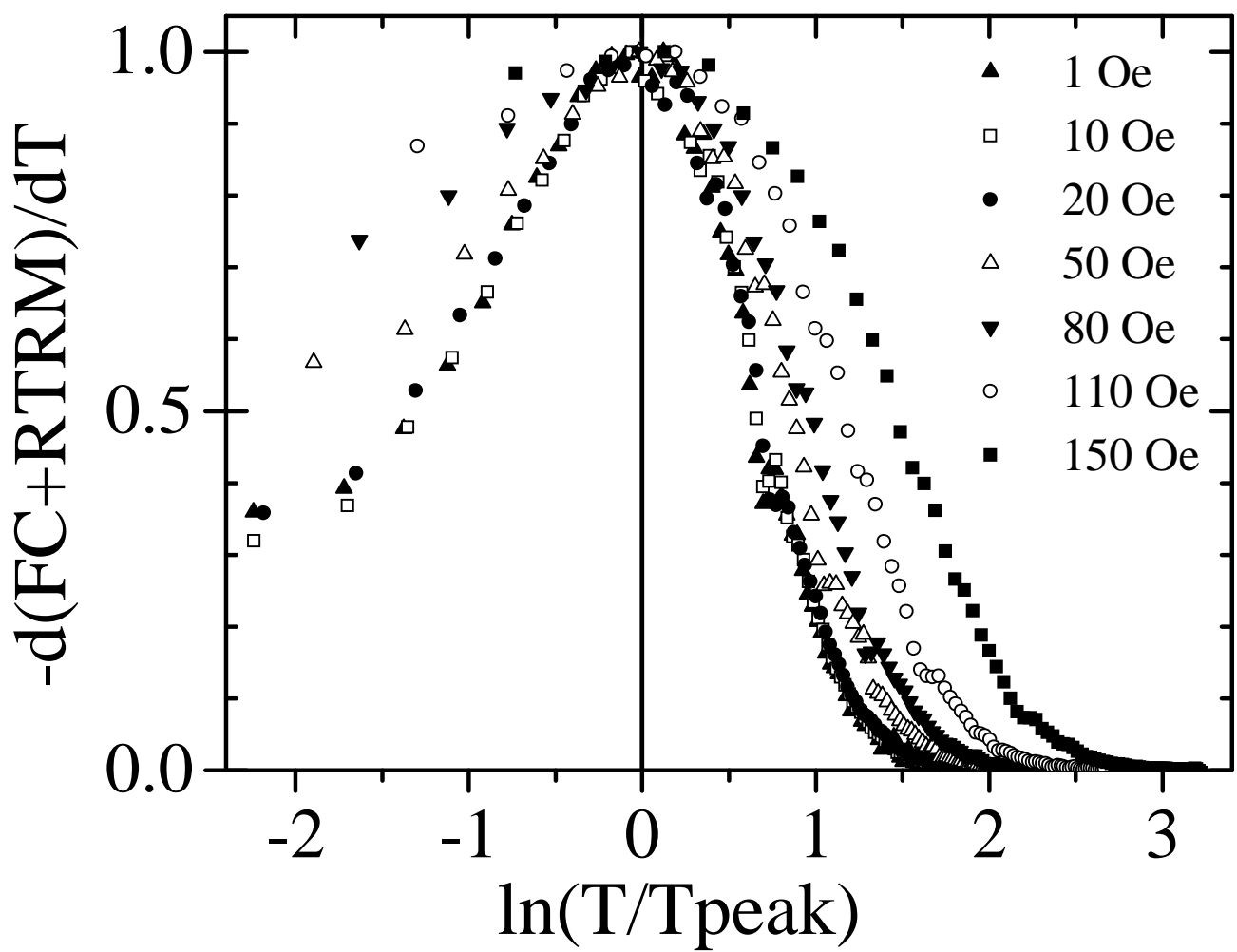


Fig. 7

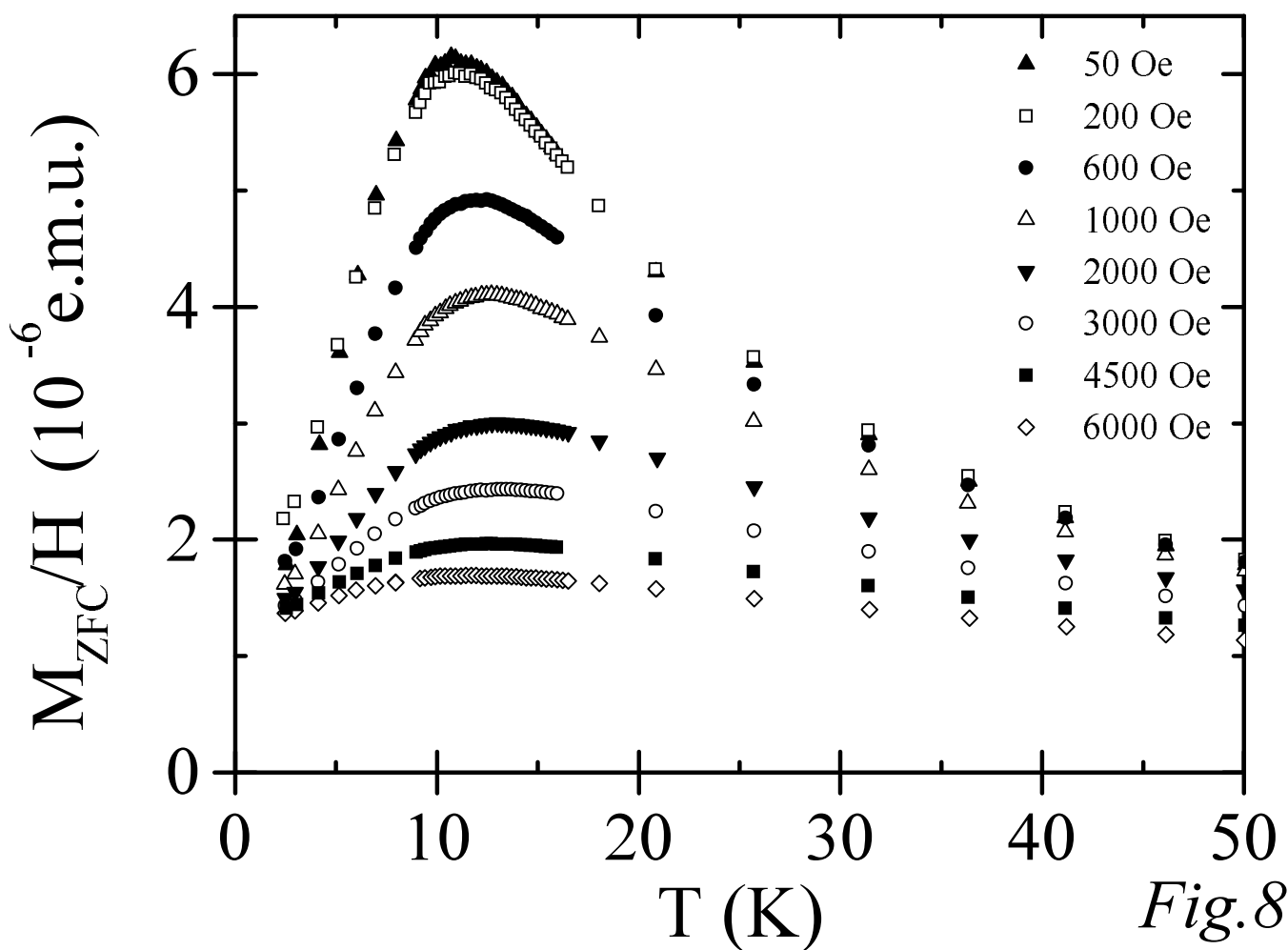


Fig.8a

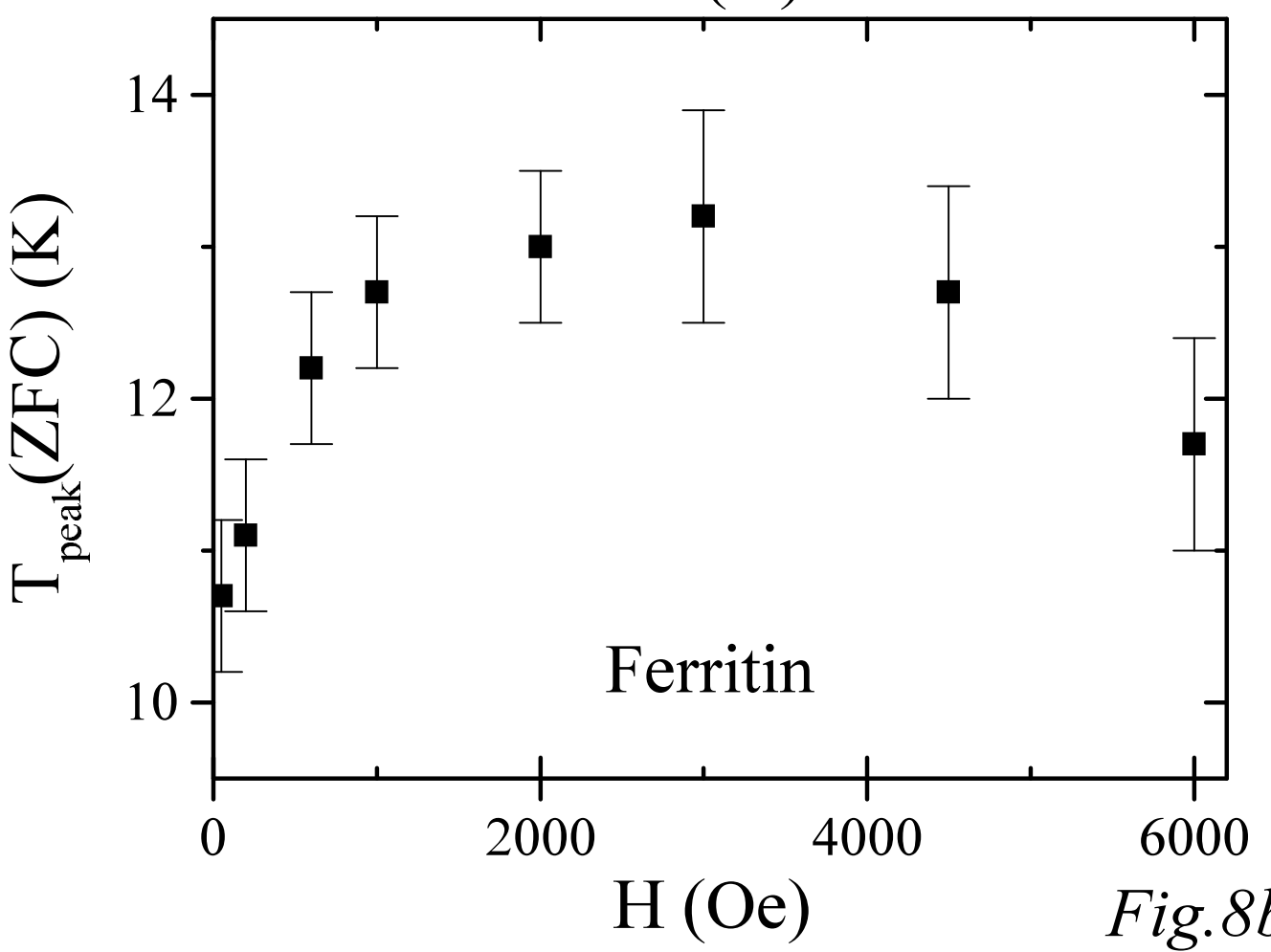


Fig.8b

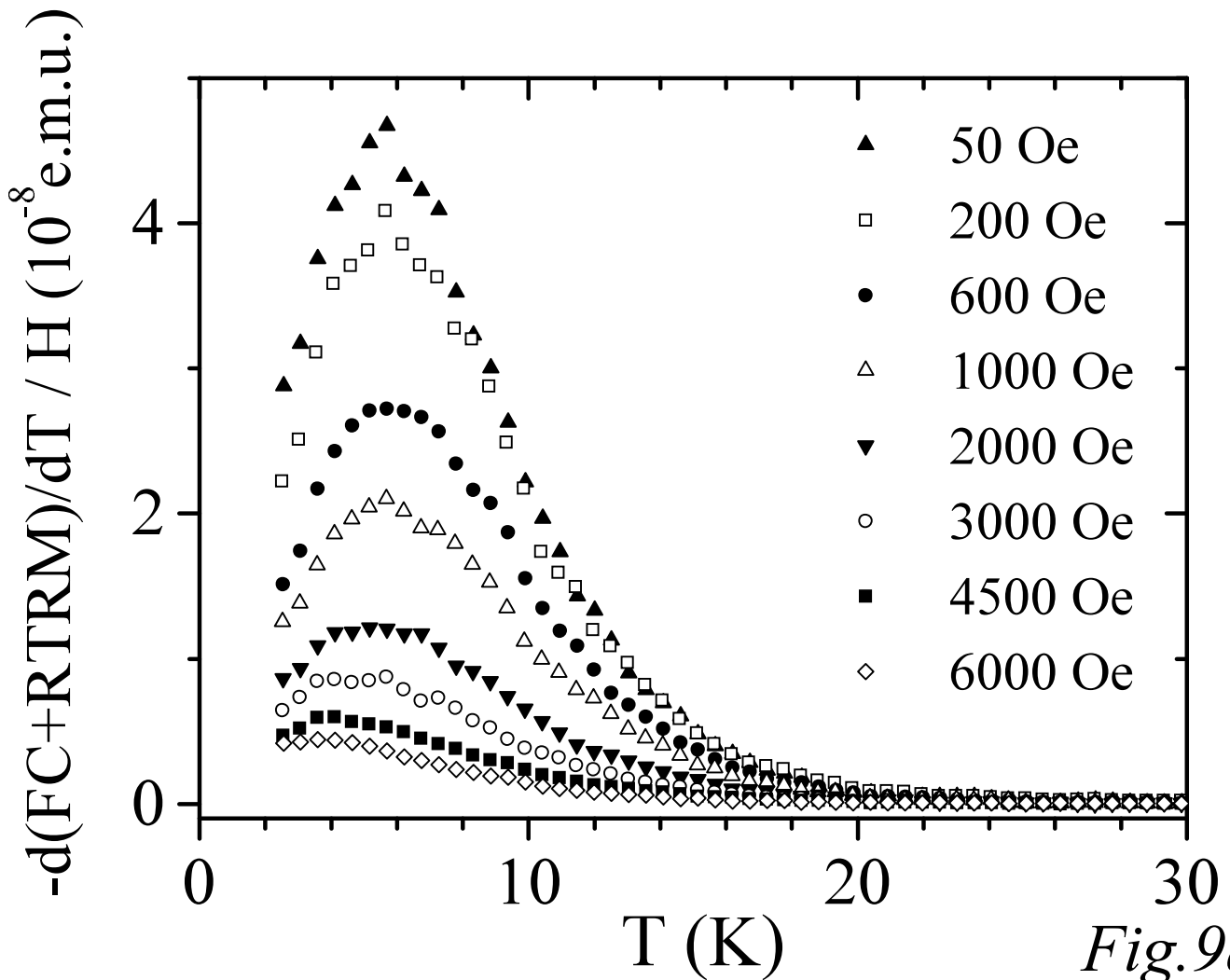


Fig. 9a

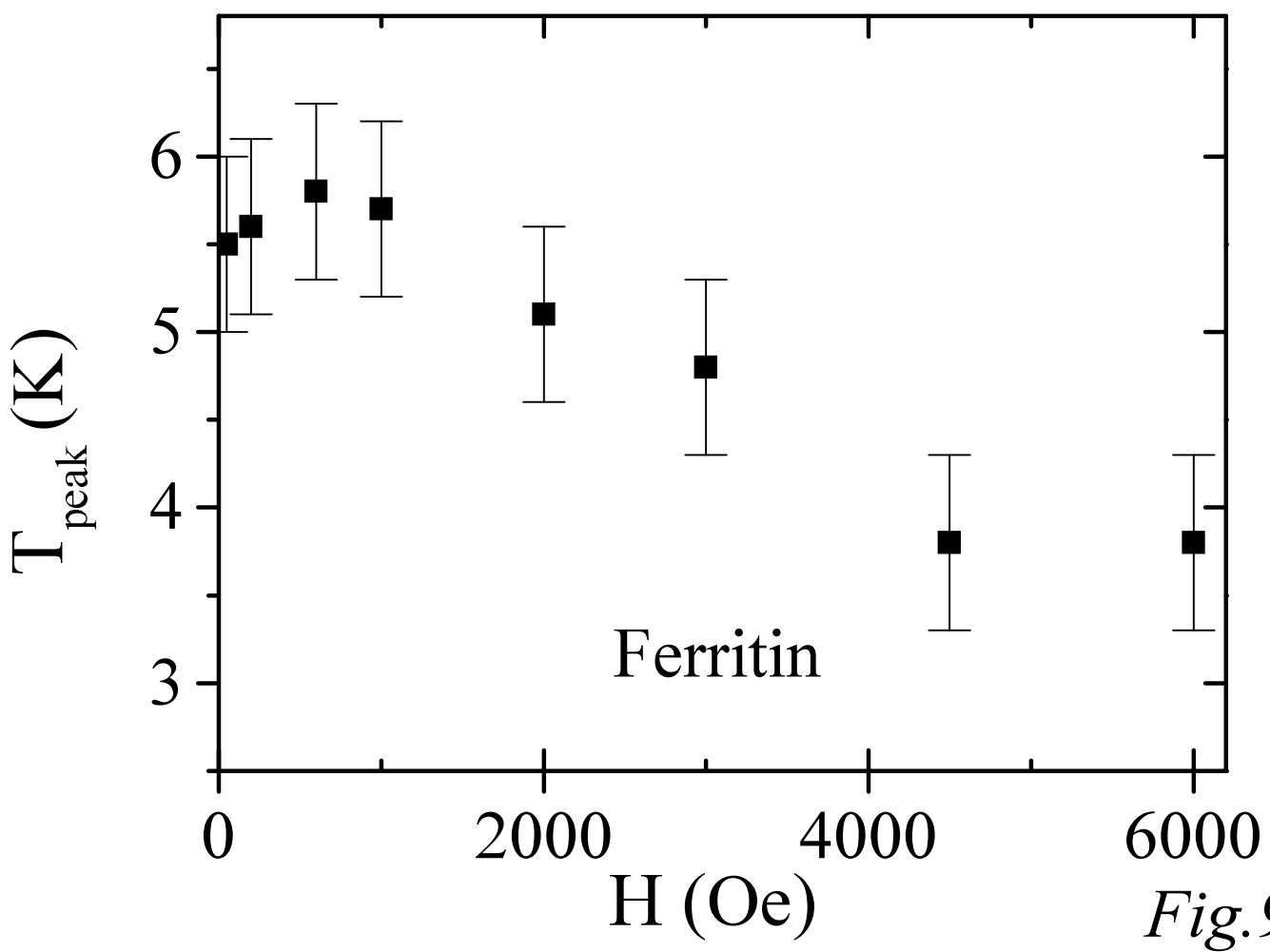


Fig. 9b

